minerals

MDPI

Article

An Isotope Study of the Dzhida Mo–W Ore Field (Western Transbaikalia, Russia)

German S. Ripp, Olga K. Smirnova, Ivan A. Izbrodin, Eugeny I. Lastochkin, Mikhail O. Rampilov * and Viktor F. Posokhov

Geological Institute, Siberian Branch of the Russian Academy of Sciences, Sakh'yanovoi st. 6a, 670047 Ulan Ude, Russia; ripp@ginst.ru (G.S.R.); meta@ginst.ru (O.K.S.); izbrodin@ginst.ru (I.A.I.); last@ginst.ru (E.I.L.); vitaf1@yandex.ru (V.F.P.)

* Correspondence: rampilov@ginst.ru; Tel.: +7-301-2433955

Received: 27 September 2018; Accepted: 21 November 2018; Published: 24 November 2018

Abstract: The Dzhida ore field includes Pervomaika (Mo), Inkur (W) and Kholtoson (W) deposits. This article presents stable and radiogenic isotopic data (O, C, D, S, Sr and Nd) in an attempt to better understand the petrogenetic processes and the problem concerning the sources of ore-forming fluids. Granites from the Pervomaika deposit, which includes Mo-ores, as well as the syenite dikes that precede W-mineralization, have low $\delta^{18}O$ values (about 5‰ and 4‰ respectively), and low initial ratios $^{87}Sr/^{86}Sr$ (0.704–0.705). The εNd (T) values (+0.9−−1.1) in granites and syenites are close to the evolution trend of the mantle-derived source. It was determined that a mantle-derived source was involved in ore-forming processes. It was also confirmed that $\delta^{34}S$ values in sulfide minerals (molybdenite, pyrite, sphalerite, galena, and chalcopyrite) were close to the meteoric standard (from −2‰ to +2‰). The $\delta^{13}C$ and $\delta^{18}O$ values in carbonate minerals (rhodochrosite and ankerite) of the Kholtoson deposit are located within the primary igneous carbonatite (PIC)-square, as a possible juvenile source of CO_2. This was also confirmed by the $\delta^{18}O$ and δD values in muscovite from greisens (4.2‰–6.5‰ $\delta^{18}O$, –78.8‰ … –84.0‰ δD). The $\delta^{18}O$ values calculated in a fluid equilibrated with hydrothermal minerals indicated a meteoric origin.

Keywords: Mo–W deposits; oxygen isotopes; fluid source; Western Transbaikalia

1. Introduction

The Dzhida ore field is a large Mo–W deposit in Russia (1.4 Mt of WO_3 and 1.7 Mt of MoO_3). It has been studied by many researchers. However, the problem of the sources of ore-forming fluids has not been investigated. Limited complex isotope studies of Mo–W deposits have been carried out in deposits in China [1–6], Kazakhstan [7], and Russia [8–10]. Our study presents stable and radiogenic isotopic data (O, C, D, S, Sr and Nd) in an attempt to better understand the petrogenetic processes and the problem concerning the sources of ore-forming fluids.

It is well known that rare metal mineralization is usually associated with granitic rocks. Researchers consider that mineralization could be formed by several mechanisms. In one case, it occurs due to the intensive differentiation of a standard granite melt [11–13], while in another case it is expected to occur due to the transport of elements to the apical part of a magmatic chamber [14], or as a result of special melting conditions and the involvement of special sources of fluids [15,16]. Some researchers have proposed that metasomatic processes caused a redistribution of rare metals [17,18]. All of these models are based on the similarity between the chondrite-normalized Rare Earth Elements (REE) patterns of host rocks and ore-mineralization zones or on the comparison between the mineral and/or chemical composition of the host rocks and the ores. Some researchers have studied fluid inclusions and used initial $^{87}Sr/^{86}Sr$ ratios to show the relationship between the ores and the host

rocks. However, all of these models suggest a crustal-derived source of the fluids because the ore mineralization zones are located within/or near granite massifs.

According to isotopic investigations, ore mineralization is not always formed due to the fractional crystallization of igneous rocks. It is considered that metamorphic, juvenile, and meteoric fluids were involved in the formation of some deposits related to igneous rocks. The fluids were able to escape during the boiling of the melt. Some deposits related to skarns formed with the participation of fluids with low δD (meteoric water) values [19]. The role of such waters increased up to the final phase of the ore formation. The recycling of meteoric water caused by granite plutons is expected in the formation of apocarbonate nephrites [20], the REE-mineralization of the Songwe Hill carbonatites [21], and the Be-mineralization of the Spor Mountain deposit [22,23].

As large Mo–W deposits are located close to granitic rocks, the hypothesis of a crustal-derived source in deposits is prevalent. An important feature of the Transbaikalia region, where the Dzhida ore field is located, is the presence of the Late Mesozoic rifting zone related to basalts. Several granitic and alkaline massifs, the Central Asian fluorite belt, the Western Transbaikalian Carbonatite Province, and a large amount of Mo–, and Mo–W-deposits related to granites, were formed during this period.

Sheglov [24] suggested that fluids from a deep source participated in the formation of the deposits. This assumption is proved by the $\delta^{34}S$ values [25,26] and the Sr-Nd isotopic values [8] in the Dzhida deposit. Some deposits have high $\delta^{34}S$ values, and a low amount of fluorite and sulfides is, therefore, formed by the crustal-derived source. They are of small industrial significance. The other deposits have $\delta^{34}S$ values close to the mantle-derived source and are industrially significant (i.e., Dzhida, Orekitkan, and Buluktai). There is a high concentration of fluorite and sulfides [26].

2. Geological Background

The Dzhida ore field is located in the Western Transbaikalia and includes the Pervomaika Mo-deposit, the Inkur, and the Kholtoson Mo–W deposits. Earlier studies have focused on describing the geology and mineral compositions of the ores and their relationship to country rocks and PT-parameters [27–33].

The Dzhida ore field is located in Early Paleozoic crystalline schists, Caledonian quartz diorites, and granodiorites (Figure 1). There is a stock of granite porphyry (the Pervomaika massif) and dikes of aplites, plagiogranites, syenites, quartz syenites and diorites within the ore field. The country rocks are serpentinized ultrabasites.

According to the Rb–Sr investigation [5] and geological observations, a sequence of events is supposed: (1) the addition of the Pervomaika granites 124.3 ± 1.6 Ma; (2) greizenization 123.5 ± 0.7, and; (3) hydrothermal W–Mo stage 123 ± 0.3. More precise methods have given different results: 121 Ma (U-Pb SRIMP II, zircon)—the addition of the Pervomaika granites [34], and 115.9 (Ar-Ar, biotite)—the addition of the syenites preceding the W–Mo stage.

All deposits of the Dzhida ore field were formed in two stages: (1) molybdenum is the early stage, and (2) tungsten is the late stage. There are some mineral associations in each stage. The fluorite–muscovite greisens were formed after the addition of the Pervomaika granites to the apical part of the massif during the postmagmatic stage. The Mo-mineralization is presented by stockwork and is mostly located within the Pervomaika massif of the granites and partly in the host crystalline schists. The molybdenite, quartz–molybdenite and quartz–K-feldspar–beryl veinlets (the Pervomaika stockwork) cut the fluorite–muscovite greisens. The molybdenum stage is finished by the addition of aplites. All veinlets of the molybdenum stage are cut by the dikes of syenites followed by W-bearing veins and veinlets—the tungsten stage. The Inkur stockwork and the Kholtoson veins were formed during this stage after the dikes of syenites. The tungsten stage is divided into three substages. The earliest are quartz-K-feldspar-hubnerite veinlets containing muscovite, fluorite, and beryl (the Inkur stockwork) followed by quartz-sulfide-hubnerite and quartz–carbonate–hubnerite veins (the Kholtoson). The main ore-forming minerals of the W-stage are quartz and hubnerite. Most of the sulfides are located in quartz–sulfide–hubnerite veins and are presented by pyrite,

sphalerite, galenite, and sulfosalts of bismuth. Additionally, there are triplite, fluorite and muscovite. The latest substage is presented by quartz–carbonate–hubnerite veins containing rodochrosite, ankerite and calcite.

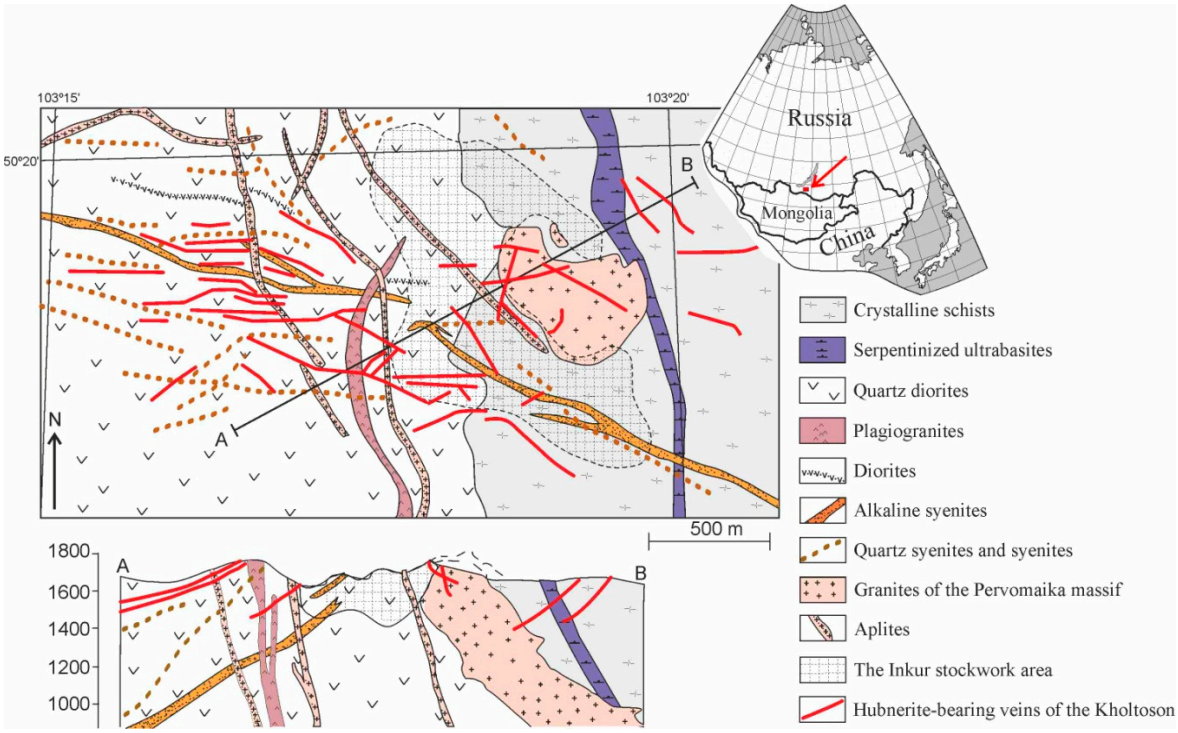

Figure 1. Geological sketch map and cross section of the Dzhida ore field after Ignatovich, 2007 [32]. The inset map shows the location of the Dzhida ore field.

2.1. The Pervomaika Deposit

The Pervomaika Mo-deposit includes stockworks of differently oriented molybdenite and quartz–molybdenite veins, which cut the granite massif and partly cut country rocks. The stockwork area on the surface is 620 × 540 m and it is traced to a depth of 240–250 m. The massif is a fractured intrusion, confined to the tectonic zone of the north-western strike, with a gentle declination under the volcanic–sedimentary series. Its crystallization temperatures [35,36] are in the range of 750–800 °C. The massif consists of granites and granite porphyry containing about 75 wt. % SiO_2, 15.5 wt. % Al_2O_3, 9 wt. % $Na_2O + K_2O$, with a predominance of K_2O over Na_2O and low concentrations of TiO_2, MgO, and Fe_2O_{3tot}. The apical part of the massif includes porphyry phenocrysts of quartz.

The massif is cut by biotite–quartz, quartz–feldspathic veins, and pegmatites. The massif has undergone K-feldspathization and greisenization. There are mica-bearing greisens containing high concentrations of fluorite in the apical part of the massif. With depth, the intensity of the greisenization decreases, and at a depth of about 200 m biotitic granites with a high concentration of albite appear. In the contact zones with the crystalline schists, hornfelses are common.

There are molybdenitic and quartz–molybdenitic veins within the granitic stock (Figure 2), and rarely outside. These veins often contain fluorite, pyrite, K-feldspar, muscovite, and beryl. Stringer mineralization with veinlets from 1 mm to 5 cm in thickness (in some cases 10–30 cm), accompanied by zones of disseminated Mo-mineralization, is of great economic interest. The main body of the Pervomaika stockwork is filled with ore containing 0.10–0.15% Mo. The Pervomaika stockwork is cut by the dikes of alkaline and quartz syenites. The homogenization temperatures of the fluid inclusions from quartz of the initial stage vary from 240 to 280 °C [30]. In the inclusions of the later stage, the homogenization temperatures are in the range 250–200 °C, and a high concentration of CO_2 is recorded in the gas phase. The areas of greisenization and molybdenite-bearing veins are cut by the dikes of

aplite, syenite and quartz syenite. Apart from this, there are hubnerite-bearing veins with carbonates and sulphides in the area of the deposit. Sulfide (main mineral is molybdenite) and oxidized ores (main mineral is ferrimolybdite) hosted in granite and slate are separated in the Pervomaika. Only sulfide ore hosted in granite was mined earlier. About 17,000 t of molybdenum concentrate has been output. Owing to a lack of concentration technology, the oxidized ore hosted in the granite and country slate, as well as the sulfide-bearing slate ore, were stored in a special dump. The deposit was mined in 1941–1973.

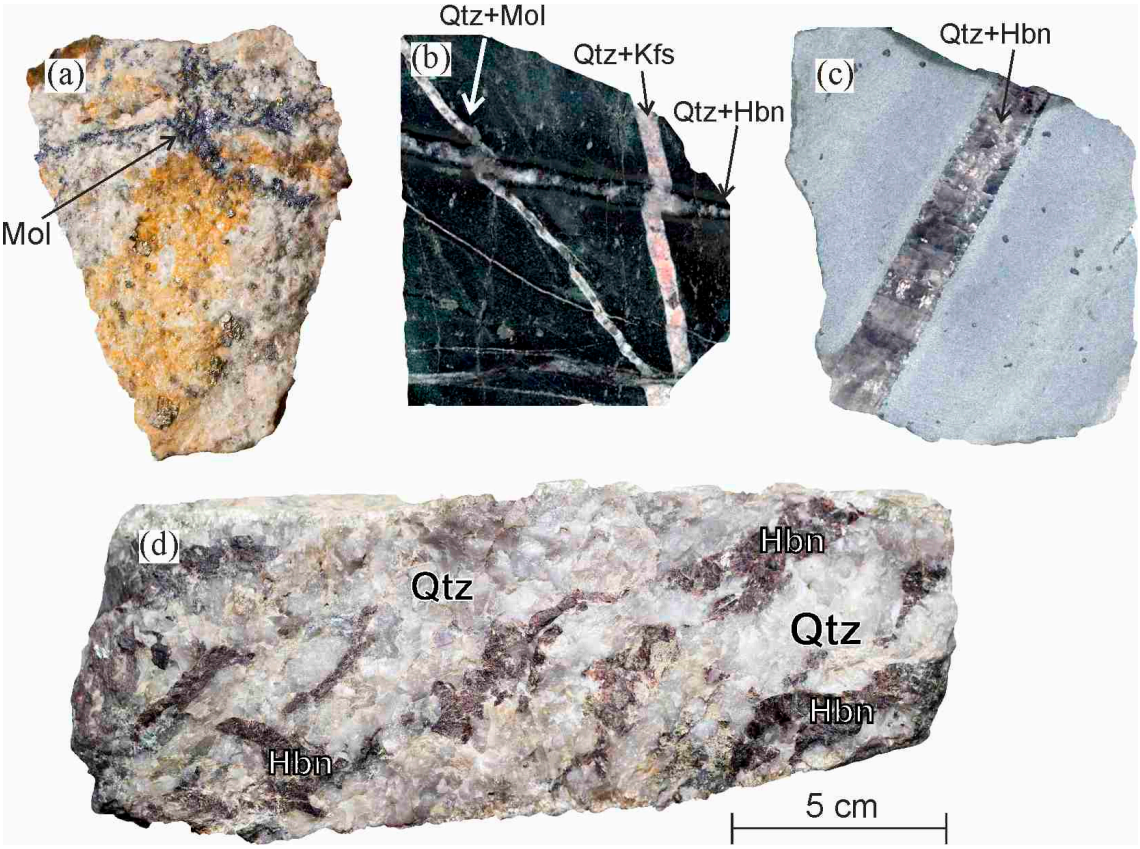

Figure 2. Photos of typical ore-samples from the Dzhida ore-field. (**a**) Molybdenitic vein cutting through the Pervomaika granite (sample P-15-2); (**b**) quartz-hubnerite vein cutting through the quartz–molybdenite vein. All the veins cut through the crystalline schist (the Inkur deposit) (sample 105-78); (**c**) quartz–hubnerite vein cutting through the dike of alkaline syenite (the Inkur deposit) (sample 110); (**d**) hubnerite grains within quartz (the Kholtoson) (sample Dzh-1). Mol—molybdenite, Hbn—hubnerite, Otz—quartz, Kfs—K-feldspar.

2.2. The Inkur Deposit

The Inkur W-deposit is located in the exocontact zone of the Pervomaika massif as a wide half ring, which surrounds the massif in the south–west, west, and north–west area (see Figure 1). The deposit is localized mainly in quartz diorite and partly in crystalline schists. The deposit is a stockwork extending for 2500 m, with a width of 800–850 m, and a depth of 470–500 m. The W-mineralization is represented by numerous quartz and quartz–feldspar veinlets containing hubnerite, scheelite, fluorite, beryl, pyrite, sphalerite, galena and sulfosalts of bismuth and silver. These veins were formed after the dikes of syenites and the Pervomaika granites and cut them all (see Figure 2). The veins are also enriched by fluorite. The hubnerite and beryl tend to be mainly located at the contacts of the veins, but sulphides are located in the central zones. The homogenization temperatures of fluid inclusions from quartz are in the range of 200–350 °C [30]. The W-mineralization is distributed non-uniformly. The enriched areas are located on the southern and northern flanks, whereas the central part of the mineralization is

relatively low-grade. The relationship of ore strips with different orientations results in an increase in their thickness with the formation of blocks that are complex in shape, which are enriched in WO_3 up to 0.16–0.18%. The average concentration of WO_3 throughout the stockwork is rather stable (0.147%).

2.3. The Kholtoson Deposit

The Kholtoson W-deposit is located west of the Inkur deposit at the distance of the Pervomaika massif and features hydrothermal quartz–hubnerite veins with a variable amount of sulphides. Approximately 32,800 t of tungsten concentrate was mined. There are widespread dikes of syenites, quartz syenites, and alkaline syenites in the area of the deposit. The syenites have biotite as a dark-colored mineral, and the alkaline syenites have arfvedsonite. The quartz–hubnerite veins were formed after the addition of the syenite dikes, like the Inkur stockwork. All the quartz–hubnerite veins form a strip elongated in the sublatitudinal direction, spatially coinciding with the field of the dikes. There are about 150 quartz–hubnerite veins ranging from tens of centimeters to 2–4 m (up to 6–12 m when blown out) in thickness and up to several hundred meters in length. The veins are traced to a depth of 600–650 m, cut quartz diorites and crystalline schists, and are also found in granites in the Pervomaika massif. The veins are rimed by muscovite. The veins were formed due to the filling of the fractures and were accompanied by pyritization and greisenization. There are quartz–hubnerite and quartz–sulphide–hubnerite veins (see Figure 2). In general, throughout the deposit, the WO_3 content is 0.77%. The mineral composition is similar to that of the Inkur stockwork, characterized by a large amount of sulphide minerals such as pyrite and less sphalerite, galena, chalcopyrite and sulfosalts of bismuth. Moreover, apatite, triplite, and some carbonates (rhodochrosite, ankerite, calcite, siderite and dolomite) are present as accessories. The rhodochrosite was formed after the hubnerite and before the sulfides. The calcite formed at the latest stage of hydrothermal alteration. The hubnerite is partly altered by scheelite. One of the earliest minerals is triplite, which is altered by rhodochrosite. The important feature of the Kholtoson deposit is that it is enriched by Mn. There are many Mn-bearing minerals such as hubnerite, rhodochrosite, triplite, dolomite, siderite-(Mn), apatite (containing up to 2 wt. % MnO), and ankerite (6–15 wt. % MnO). The homogenization temperatures of the fluid inclusions from quartz and sphalerite range from 150–350 °C and are close to those of the Inkur stockwork [29–32]. However, the temperatures of the initial stage (the formation of W-mineralization) are in the range of 280–350 °C.

3. Analytical Methods

The oxygen and carbon isotopic compositions were analyzed at the Geological Institute of the Siberian Branch of the Russian Academy of Sciences and at the Center for Isotopic Research of the Far East Science Center of the Russian Academy of Sciences. The oxygen in the silicates was analyzed using laser fluorination, while the carbon and oxygen in the carbonates were analyzed using the technique of decomposition by orthophosphoric acid with a "Gasbench" option at 60–70 °C for 2–4 h. All the measurements were carried out on a Finnigan MAT 253 mass spectrometer (ThermoFinnigan, Bremen, Germany) using a double inlet system for oxygen in silicates and a "continuous helium flow" for carbonates. The measurements were calibrated using international standards NBS-28 (quartz), NBS-30 (biotite) [37] for silicates and NBS-18 and NBS-19 [38] for carbonates. The VPDB (Vienna-Pee Dee Belemnite) standard is used. The error of the values obtained did not exceed 0.2–0.3‰.

The oxygen isotopic composition in the fluids was estimated by means of a program for isotope equilibrium calculation [39], using coefficients of equilibrium fractionation for each mineral [40–43] and the temperatures obtained during the thermobarogeochemical studies.

The hydrogen isotopic composition in the hydroxyl-bearing minerals was determined at the Center for Isotope Research of the Far East Science Center of the Russian Academy of Sciences using the method described in Reference [44]. The samples were preliminarily heated up to 200 °C to remove sorbed water. Constitutional water was released at 1250 °C. Hydrogen was extracted from water on chromium at 950 °C. Its isotopic composition was analyzed using a Finnigan MAT 253 mass

spectrometer with respect to the laboratory standard calibrated against VSMOW (Vienna Standard Mean Ocean Water), SLAP (Standard light Antarctic Precipitation), and GISP (Greenland Ice Sheet Precipitation) international standards. The reproducibility of the δD (1σ) measurements was 1.5‰.

The sulfur isotopic composition in the sulfides was measured at the Center for Isotope Research of the Far East Center of the Russian Academy of Sciences. Samples for mass spectrometric isotope analysis of sulfur were prepared using the technique by Reference [45]. Sulfide sulfur was oxidized to SO_2 using copper oxide. Oxidation was carried out under vacuum at 900 °C. The SO_2 obtained was purified from other reaction products using a thermally regulated cryogenic trap. The purified SO_2 was frozen in an individual ampoule. The sulfur isotope ratios were measured using a Finnigan MAT 253 mass spectrometer with a double inlet system. The measurement error of $\delta^{34}S$ (1σ) was 0.1‰. The CDT standard (Vienna-Canyon Diablo Troilite) is used.

The isotopic composition of Nd and Sr was measured using a Triton multichannel mass spectrometer in a static regime at the Institute of Precambrian Geology and Geochronology RAS, St. Petersburg, Russia. The method of preparation for the Nd and Sr isotope investigations was described by Reference [46]. The reproducibility of the determinations of the Rb, Sr, Sm, and Nd isotopic compositions was estimated to be ±0.5% from the replicate analyses of the BCR (Basalt, Columbia River) standard. The total blanks were 0.05 ng for Rb, 0.2 ng for Sr, 0.3 ng for Sm, and 0.8 ng for Nd. The results of the analysis of a standard BCR-1 sample (6 measurements) were as follows: Sr = 336.7 μg/g, Rb = 47.46 μg/g, Sm = 6.47 μg/g, Nd = 28.13 μg/g, $^{87}Rb/^{86}Sr = 0.4062$, $^{87}Sr/^{86}Sr = 0.705036 \pm 22$, $^{147}Sm/^{144}Nd = 0.1380$, $^{143}Nd/^{144}Nd = 0.512642 \pm 14$. The reproducibility of the isotope analyses was evaluated using the measurements of the La Jolla and SRM-987 standards. Concurrently with the Sr measurements, the $^{87}Sr/^{86}Sr$ ratio in the SRM-987 standard was found to be 0.710241 ± 15 (2σ, 10 measurements), whereas the value of $^{143}Nd/^{144}Nd$ in the La Jolla standard was 0.511847 ± 8 (2σ, 12 measurements). The Sr isotope composition was normalized to $^{88}Sr/^{86}Sr = 8.37521$, whereas the Nd composition was normalized to $^{146}Nd/^{144}Nd = 0.7219$. The Nd isotope composition was corrected to $^{143}Nd/^{144}Nd = 0.511860$ in the La Jolla standard.

The microtextural features, relations, and homogeneity of the minerals were studied using a LEO-1430 electron microscope equipped with EDS (Energy Dispersive Spectroscopy) Inca Energy using the facilities of the "Analytical Center of Mineralogical, Geochemical and Isotope Studies" at the Geological Institute, SB RAS Ulan-Ude, Russia.

4. Results

4.1. O, C, H Isotope Data

4.1.1. The Pervomaika Deposit

The granites, greisens (muscovite), and hydrothermal veins (quartz, muscovite, beryl and K-feldspar) were studied (Table 1). The quartz and K-feldspar from the Pervomaika granites had lower $\delta^{18}O$ values than that of the Western Transbaikalia [47–49]. The quartz from the molybdenite-bearing veins and the mica from the greisens had similar $\delta^{18}O$ values, but the beryl and the K-feldspar from the veins had higher $\delta^{18}O$ values. The calculated $\delta^{18}O$ values of fluid, which are in equilibrium with the muscovite from the greisens, showed that a mantle-derived source participated in the formation process. This was also confirmed by the δD (−78.8‰) values in the muscovite.

Table 1. The $\delta^{18}O$ values in minerals from the Pervomaika deposit.

ID No.	Sample No.	Description	Mineral	$\delta^{18}O$‰	$\delta^{18}O$‰	Proportion of Meteoric Water (%)
				VSMOW	Fluid	
Granite (750 °C)						
1	P-15-1a	Euhedral grains	Quartz	5.9	4.6	13.7
2	P-15-1б	Interstitial grains	K-feldspar	5.3	5.3	11.2
3	P-15-2a	Euhedral grains	Quartz	5.5	4.2	15.1
4	P-15-2б		K-feldspar	4.7	4.7	13.3
Pre-ore stage (Greisen, 350 °C)						
5	P-15-9	Aggregates of dense bladed crystals	Muscovite	7.3	6.7	6.3
Hydrothermal stage (350 °C)						
6	P-15-7	Lamellar aggregate from quartz–molybdenite veins	Muscovite	3.9	3.3	18.3
7	P-17-1		Muscovite	4.8	4.2	15.1
8	P-15-7б	Euhedral grains from quartz–K-feldspar–beryl veinlets	K-feldspar	3.8	0.7	27.4
9	P-15-6		K-feldspar	5.4	2.3	21.8
10	P-15-7a		Beryl	4.5	5.0	12.3
11	P-17-2		Beryl	5.3	5.8	9.5
12	P-15-1		Quartz	6.5	0.9	26.7
13	P-15-2/1		Quartz	5.3	−0.3	30.9
14	P-15-3	Quartz–molybdenite veinlets	Quartz	5.7	0.1	29.5
15	P-15-4		Quartz	5.7	0.1	29.5
16	P-15-5		Quartz	6.6	1.0	26.3

The $\delta^{18}O$ values of a fluid equilibrated with minerals was calculated using quartz, K-feldspar, beryl [40] and muscovite [43]. Here and in Table 2, the meteoric water % is calculated taking into account that the $\delta^{18}O$ average value of meteoric water is −20‰, and that 8.5‰ is magmatic water.

4.1.2. The Kholtoson Deposit

The $\delta^{18}O$ values in whole-rock alkaline syenites were low (Table 2). The quartz from hydrothermal hubnerite-bearing veins had the highest $\delta^{18}O$ values among the ore-forming minerals, followed by K-feldspar. The hubnerite, triplite, scheelite and apatite had the lowest $\delta^{18}O$ values. The difference between the $\delta^{18}O$ values of coexisting quartz and hubnerite varied in the interval of 8.0–9.6‰. The temperatures calculated for this pair of minerals (277–333 °C, Table 3) were close to the temperatures obtained in thermometric studies. In the quartz–feldspar pair, the difference in the $\delta^{18}O$ values varied within the range of 1.2–2.3‰, and the temperatures calculated for them (Table 3) were somewhat higher (297–391 °C) than for the association with hubnerite.

The temperatures were calculated using $1000\ \ln a_{(A-B)} = A \times 10^6/T^2$ for pair quartz–hubnerite (Q-Hb) [24], and for pair quartz–K-feldspar (Q-Kfs) [29].

The $\delta^{18}O$ values of the fluid that participated in the formation of the greisens were close to those of a mantle-derived one. This was confirmed by the δD values of muscovite (−84.8‰ and −83.3‰). The $\delta^{18}O$ values of the ore-stage minerals were low.

The carbonates had $\delta^{18}O$ and $\delta^{13}C$ values (Table 4) close to primary igneous carbonatite (PIC-square) (Figure 3). The rhodochrosite has lower $\delta^{13}C$ values relative to the ankerite. The lowest $\delta^{18}O$ and $\delta^{13}C$ values were found in the calcite formed during the final stage of the ore formation.

Table 2. The $\delta^{18}O$ values in minerals from the Kholtoson deposit.

ID No.	Sample No.	Description	Mineral	$\delta^{18}O$‰	$\delta^{18}O$‰	Proportion of Meteoric Water (%)
				VSMOW	Fluid	
			Syenite			
1	113-46		Whole-rock	2.9		
2	KH-17		Whole-rock	4.4		
			Pre-ore stage (Greisen 350 °C)			
3	Dzh-1C	Lamellar aggregate	Muscovite	4.9	4.6	13.7
4	KH-15-6		Muscovite	5.3	5.0	12.3
5	KH-15-1		Muscovite	5.0	4.7	13.3
6	KH-15-2		Muscovite	5.5	5.2	11.6
7	KH-15-5a		Muscovite	5.3	5.0	12.28
			Ore stage (300 °C)			
8	Dzh-1к	Quartz–hubnerite veins	Quartz	7.3	0.3	28.8
9	Dzh-13/87		Quartz	8.8	1.8	23.5
10	KH-15-9a		Quartz	7.2	0.2	29.1
11	KH-15-6a		Quartz	9.7	2.7	20.4
12	KH-15-13		Quartz	8.5	1.5	24.6
13	KH-15-12/1		Quartz	7.4	0.4	28.4
14	KH-12/2		Quartz	7.8	0.8	27.0
15	KH-15-18		Quartz	9.1	2.1	22.5
16	KH-15-5		Quartz	8.7	1.7	23.9
17	KH-15-11	Quartz–carbonate–hubnerite veins	Quartz	7.3	0.3	28.8
18	KH-15-10a		Quartz	7.0	0	29.8
19	KH-15-8		Quartz	7.7	0.7	27.4
20	GM-1210		Quartz	8.9	1.9	23.2
21	KH-15-9б	Euhedral grains from quartz–hubnerite veins	K-feldspar	5.6	1.4	24.9
22	Dzh-13/87		K-feldspar	6.4	2.2	22.1
23	KH-15-8a		K-feldspar	5.7	−0.4	31.2
24	KH-15-14a		K-feldspar	5.8	1.6	24.2
25	KH-15-11a		K-feldspar	4.8	0.6	27.7
26	KH-15-10		K-feldspar	5.9	1.7	23.9
27	KH-15-7б	Euhedral grains from quartz–carbonate–hubnerite veins	K-feldspar	3.8	1.5	24.6
28	KH-15-14	Euhedral grains from quartz–hubnerite veins	Hubnerite	−1.1	0.7	27.4
29	Dzh-1в		Hubnerite	−0.7	1.1	26.0
30	KH-15-13		Hubnerite	−1.1	0.7	27.4
31	KH-15-15		Hubnerite	−2.7	−0.9	33.0
32	KH-15-10		Hubnerite	−2.5	−0.7	32.3
33	GM-12-10	Euhedral grains from quartz–carbonate–hubnerite veins	Hubnerite	−0.9	0.9	26.7
34	P-15-9a		Hubnerite	−1.4	0.4	28.4
35	P-18-4		Hubnerite	−1.4	0.4	28.4
36	Dzh 13/87		Triplite	1.5		
37	Dzh-2		Triplite	1.1		
38	GM-1210		Scheelite	1.9	−0.8	32.6
39	P-18-2		Apatite	2.6		
40	P-18-4		Apatite	1.9		

The $\delta^{18}O$ values of a fluid equilibrated with minerals were calculated using hubnerite [41] and scheelite [42]. The temperature was 200 °C.

Table 3. Temperatures calculated and $\delta^{18}O$ values in coexisting mineral pairs from the Kholtoson deposit.

Sample	GM-1210	KH-15-10a	KH-15-13	KH-15-9a	KH-15-5	Sample	KH-15-8	Dzh-13/87	KH-15-11
Quartz	8.9	7.0	8.5	7.2	8.7	Quartz	7.7	8.8	7.3
Hubnerite	−0.9	−2.5	−1.1	−1.4	−1.1	K-feldspar	5.7	6.4	4.8
Δ	9.8	9.5	9.6	8.6	9.8	Δ	2.0	2.4	2.5
T (Q-Hb)	277	290	286	333	281	T(Q-Kfs)	391	313	297

Table 4. The $\delta^{18}O$ and $\delta^{13}C$ values in carbonate minerals from the Kholtoson deposit.

Sample No.	Mineral	$\delta^{18}O$, ‰ VSMOW	$\delta^{13}C$, ‰ VPDB
Dzh-1	Rhodochrosite	9.3	−7.0
23/4	Rhodochrosite	6.8	−5.7
P-1	Rhodochrosite	7.8	−7.5
P-2	Ankerite	9.2	−4.4
P-16	Ankerite	9.8	−4.2
KH-15-18	Ankerite	8.14	−3.8
1300	Calcite	5.8	−8.9

All samples were collected from the quartz–carbonate–hubnerite veins.

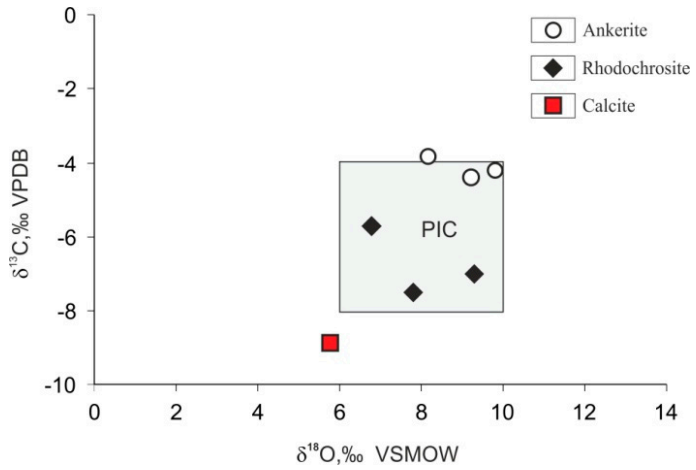

Figure 3. Diagram of the $\delta^{18}O$ vs. $\delta^{13}C$ values for carbonates from the Kholtoson deposit. PIC—primary igneous carbonatite field after Reference [50], Taylor et al., 1967.

4.2. S Isotope Data

The sulfur isotopic compositions of the sulfide minerals are given in Table 5. The sulphides of all three deposits were characterized by $\delta^{34}S$ values similar to the meteoritic standard. Some samples had negative $\delta^{34}S$ values. The molybdenites from the Pervomaika deposit had higher $\delta^{34}S$ values than pyrites. The galena from the Kholtoson deposit had low $\delta^{34}S$ values.

Table 5. The $\delta^{34}S$ in the sulfide minerals in all deposits from the Dzhida ore field deposit.

Sample No.	Description	Mineral	$\delta^{34}S$‰ VCTD
	The Pervomaika deposit		
201/1	Blade crystals from quartz–molybdenite veinlets	Molybdenite	2.1
201/2		Molybdenite	0.3
201/3		Molybdenite	1.5
C-160	Blade crystals from molybdenite veinlets	Molybdenite	−0.2
P-17		Molybdenite	−0.2
P-C-223	Euhedral crystals from quartz–molybdenite veinlets	Pyrite	−1.3
P-C-223-1		Pyrite	−1.8
P-C-228		Pyrite	−0.9
P-C-123		Pyrite	0.9
P-C-123-1a		Sphalerite	−1.9
P-C-123-2		Sphalerite	1.1

Table 5. *Cont.*

Sample No.	Description	Mineral	$\delta^{34}S$‰ VCTD
	The Inkur deposit		
105-78	Euhedral crystals from quartz–K-feldspar–hubnerite veinlets	Pyrite	−0.7
105-78-1		Sphalerite	−2.2
105-78-2		Chalcopyrite	1.2
	The Kholtoson deposit		
1615-4	Euhedral crystals from quartz–sulfide–hubnerite veins	Pyrite	0.3
1370-6		Pyrite	2.4
182-383		Pyrite	2.3
C-33-182		Pyrite	1.3
247-1		Sphalerite	2.2
1370		Chalcopyrite	−0.4
1370-1	Euhedral grains from quartz–carbonate–hubnerite veins	Galena	−5.3
C-105-15		Galena	1.5
1700		Galena	−0.9
247		Galena	−1.8
247-1a		Galena	−1.8
1789		Galena	−6.0

4.3. Sr, Nd Isotope Data

The Sr-Nd-Sm isotope data were determined in the Pervomaika granite and dikes of syenites. They had low initial ratios of Sr_i = 0.704–0.705 and εNd (T) values close to the evolution trend of the mantle-derived source. The minerals from the Kholtoson veins (fluorite and carbonates) had Sr_i values ranging from 0.7047 to 0.7055 [8]. The minerals from the hydrothermal stage as well as the igneous rocks had positive εNd (T) values (fluorite ranging from +0.1 to +3.3, and hubnerite, K-feldspar, and calcite of +1.6, +0.4, and +3.9 respectively) and were close to the evolution trend of the mantle-derived source.

5. Discussion

Granites in the Pervomaika massif are characterized by low values of $\delta^{18}O$ (see Table 1). There are numerous data on the isotope composition of this element in granites in the Western Transbaikalia [47–49] and other regions [51], showing substantially high values of oxygen, with rare exceptions in some places.

Igneous rocks related to W-Mo ores in China and East Transbaikalia have higher $\delta^{18}O$, $(^{87}Sr/^{86}Sr)_i$ values and negative εNd (T) values [2,3] in comparison with the Dzhida ore field. The Akshatau deposit (Central Kazakhstan) is more similar to the deposits of the Dzhida ore field. Granites from the Akshatau, related to Mo-ores show restricted Sr-Nd isotopic compositions with $(^{87}Sr/^{86}Sr)_i$ values of 0.70308–0.70501 and εNd (T) values of −0.5 to +2.8. These isotopic compositions were generated by 10–30% assimilation of ancient continental material by juvenile lower crust-derived magma [7].

The $\delta^{18}O$ values in the whole-rock samples and quartz of the Dzhida deposits were mainly in the range of 10‰ to 14‰ [47]. On the territory of Western Transbaikalia, recent research [48] has pointed out the tendency for oxygen to have low values (up to 6.5‰–8‰) in massifs of a younger age. Low oxygen values are typical of granites accompanied by Mo-mineralization in the Kharitonovo deposit [47], as well as in the contents of quartz (6.7‰) and K-feldspar (3.8‰) at the Zharchiha deposit respectively. Hoefs (2009) [52] suggested that such granites could be formed from a protolith with low $\delta^{18}O$ values. Those protoliths could be basites or rocks recycled by meteoric water. In the case of granites from the Pervomaika massif, the first version cannot be supported due to the absence of xenoliths, altered basites, and any significant contamination by such elements as Cr, Ni, and Co. The model of granite formation by rocks originally enriched with low values of $\delta^{18}O$ is also uncertain.

The proportion of meteoric water involved in hydrothermal processes ranges from 7% to 33%. However, the lowest values are in greisens (6–13%). Minerals from the ore stage have been formed from a solution containing 20–30% of meteoric water (see Tables 1 and 2). Data on the isotopic composition of Sr and Nd, and the presence of mantle origin components in ores (e.g., S, F and CO_2), contradict this version. As an alternative, there is a most suitable model of granite formation in the process of rock melting under the influence of high-temperature mantle fluid flow (fluid syntexis) considered in [53]. At the same time, the presence of F in the fluid composition resulted in a decrease in the liquidus temperature. Another option could be postmagmatic hydrothermal rock alteration. In cases of postmagmatic rock alteration, we recorded sharp isotope heterogeneity within magmatic bodies.

The dikes of alkaline syenites from the Kholtoson deposit have low $\delta^{18}O$ values. Together with granites of the Pervomaika stock, this proves the specific origin of those igneous rocks.

The isotopic composition of Pb in galena is homogenous [8,26] and has $\mu = 9.3$. Low primary isotope strontium ratios and positive εNd (T) values [8] in rocks and minerals from the deposits studied suggested their direct arrival from the mantle reservoir, together with contents of F, S, and CO_2.

Their preservation, reflected by the weak contamination by crustal components, is presumably due to the limited interaction of fluids and host rocks. Transportation of elements occurred in the form of fluids when there were no significant metasomatic processes.

The isotope composition of sulfide sulfur in all three deposits of the ore field ranges within the interval typical of the meteoric standard and testifies to the participation of components of mantle origin. Such $\delta^{13}C$ values are also found in other large Mo–W deposits in Transbaikalia (Buluktai, Orekitkan, Bom-Gorkhon), which are marked by high concentrations of sulfide minerals and fluorite [25]. The isotopic compositions of sulfur in the deposits of tungsten of Central Kazakhstan (Kounrad, Karaoba, Koktenkul) [7,54] and the Kalguta molybdenum-tungsten deposit of Altai [55] are similar.

The $\delta^{18}O$ and $\delta^{13}C$ values in carbonate minerals from the Dzhida ore field are identical to unaltered carbonatites and fall into the PIC-square (see Figure 3). These values fail to support this version of the fluid involvement as a result of contamination by sedimentary carbonate rocks, and also point to the mantle origin of carbon dioxide.

Comparing the associations of the hydrothermal stages of the Pervomaika and the Kholtoson deposits, we recorded a large heterogeneity of oxygen isotope composition during the tungsten stage. The trends of isotopic oxygen composition of quartz and feldspar (Figure 4) show successive enrichment by high isotope values from granites to minerals in the W-stage. The $\delta^{18}O$ values close to igneous rocks are peculiar mainly to micas from greisens (Figure 5). The low $\delta^{18}O$ values in hubnerite, triplite, scheelite and apatite relative to the isotopic composition of quartz and K-feldspar are also due to fractionation processes.

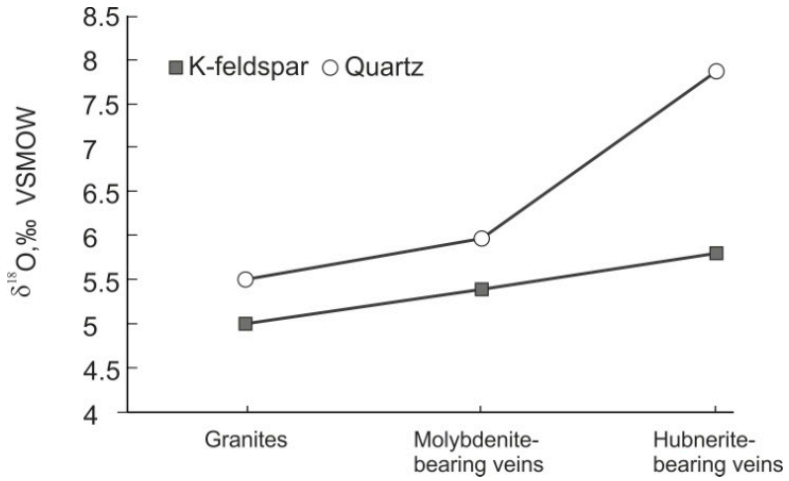

Figure 4. Evolution of $\delta^{18}O$ values in quartz and K-feldspar from granites in the Pervomaika massif molybdenite-bearing veins and hubnerite-bearing veins.

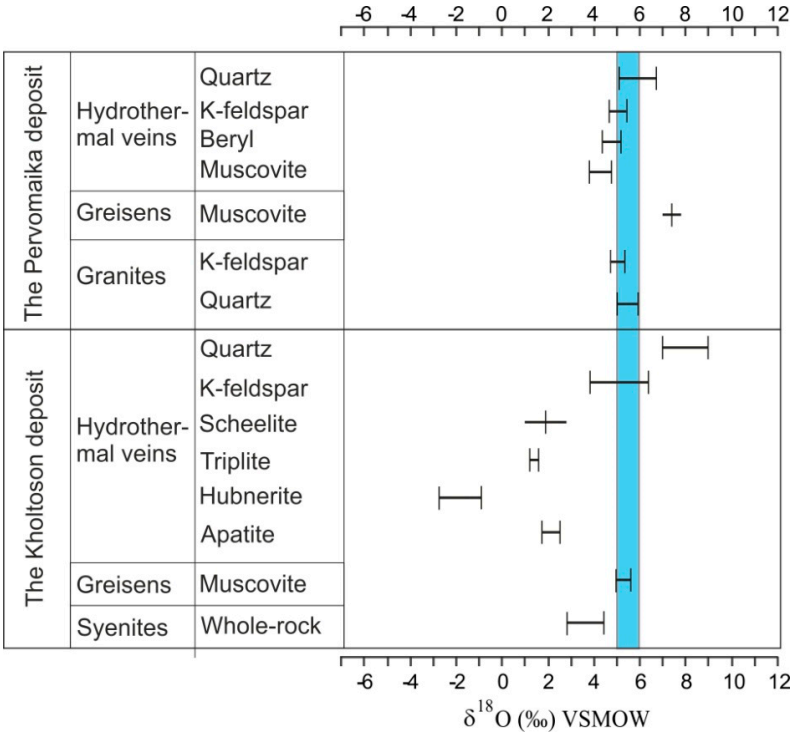

Figure 5. The $\delta^{18}O$ values in minerals from the Pervomaika and the Kholtoson deposits. The blue field within 5–6‰ $\delta^{18}O$ corresponds to the mantle oxygen values.

The temperature values calculated using the isotopic composition of hubnerite and quartz contents together (277–333 °C, see Table 3) coincided with the values obtained in experimental studies [45,46]. We obtained slightly higher temperature values (297–391 °C) for the pair with K-feldspar contents (see Table 3).

The data calculated on the oxygen composition and the degree of water depletion in micas using deuterium testify to the dominance of deep fluid during the greisen formation stage. The oxygen composition of the fluids having an equal weight to the minerals during the hydrothermal stages of both the molybdenum and the tungsten phases indicates the involvement of meteoric water in the ore formation process.

6. Conclusions

From the Sr, Nd, O, C, and D isotopic data obtained, the following conclusions can be drawn:

- Granites in the Pervomaika massif were formed as a result of the melting of the crustal substrate following exposure to high-temperature mantle fluid. The low $\delta^{18}O$ values and initial ratios of $^{87}Sr/^{86}Sr$ and the positive values of εNd (T) provide evidence of this formation.
- Components of deep (mantle) source such as F, S, and CO_2 were involved in the formation of the Dzhida ore field.
- The ore-forming fluids included waters from the meteoric source at the later stages of deposit formation.

Author Contributions: G.S.R. wrote the paper; O.K.S. collected the samples; I.A.I. and M.O.R. supported the geochemical interpretation; E.I.L. prepared the samples; V.F.P. helped write the geological settings.

Funding: This research was funded by the Russian Foundation for Basic Research, grants numbers 17-05-00129 and 16-05-01041, and project of fundamental research of RAS, grant 0340-2018-0008.

Conflicts of Interest: The authors declare no conflict of interest.

References

1. Chen, Y.-J.; Pirajno, F.; Li, N.; Deng, X.-H. Molybdenum deposits in China. *Ore Geol. Rev.* **2017**, *81*, 401–404. [CrossRef]
2. Zeng, Q.-D.; Sun, Y.; Chu, S.-X.; Duan, X.-X.; Liu, J. Geochemistry and geochronology of the Dongshanwan porphyry Mo–W. deposit, Northeast China: Implications for the Late Jurassic tectonic setting. *J. Asian Earth Sci.* **2015**, *97*, 472–485. [CrossRef]
3. Zheng, Y.; Cai, X.; Ding, Z.; Cawood, P.A.; Yue, S. Geology, geochronology and isotopic geochemistry of the Xiaoliugou W-Mo ore field in the Qilian Orogen, NW China: Case study of a skarn system formed during continental collision. *Ore Geol. Rev.* **2017**, *81*, 575–586. [CrossRef]
4. Yang, Y.F.; Li, N.; Chen, Y.J. Fluid inclusion study of the Nannihu giant porphyry Mo-W deposit, Henan Province, China: Implications for the nature of porphyry ore-fluid systems formed in continental collision regime. *Ore Geol. Rev.* **2012**, *46*, 83–94. [CrossRef]
5. Deng, X.H.; Chen, Y.J.; Santosh, M.; Wang, J.B.; Li, C.; Yue, S.W.; Zheng, Z.; Chen, H.J.; Tang, H.S.; Dong, L.H.; et al. U–Pb zircon, Re–Os molybdenite geochronology and Rb–Sr geochemistry from the Xiaobaishitou W(–Mo) deposit: Implications for Triassic tectonic setting in eastern Tianshan, NW China. *Ore Geol. Rev.* **2017**, *80*, 332–351. [CrossRef]
6. Yang, Y.; Liu, Z.-J.; Deng, X.-H. Mineralization mechanisms in the Shangfanggou giant porphyry-skarn Mo–Fe deposit of the east Qinling, China: Constraints from H–O–C–S–Pb isotopes. *Ore Geol. Rev.* **2017**, *81*, 535–547. [CrossRef]
7. Li, G.M.; Cao, M.; Qin, K.; Evans, N.J.; Hollings, P.; Seitmuratova, E.Y. Geochronology, petrogenesis and tectonic settings of pre- and syn-ore granites from the W-Mo deposits (East Kounrad, Zhanet and Akshatau), Central Kazakhstan. *Lithos* **2016**, *252–253*, 16–31. [CrossRef]
8. Chernyshev, I.V.; Gol'tsman, Y.V.; Bairova, E.D.; Ivanova, G.F. Rb-Sr geochronometry of sequential granite formation, greisenization, and hydrothermal mineralization: Evidence from the Dzhida W-Mo deposit, Western Transbaikal region. *Dokl. Earth Sci.* **1998**, *360*, 613–616.
9. Chernyshev, I.V.; Agapova, A.A.; Troitsky, V.A. Pb-Pb isotope characteristics and problem of the source of large-scale W-Mo mineralization in the Dzhida ore field (Western Transbaikalia). *Dokl. Earth Sci.* **1999**, *366*, 819–822.
10. Matveeva, S.S.; Spasennikh, M.Y.; Sushevskaya, T.M. Geochemical model of formation of the Spokininsky deposit (East Transbaikalia). *Geol. Ore Depos.* **2002**, *44*, 125–132. (In Russian)
11. Breiter, K. Nearly contemporaneous evolution of the A-and S-type fractionated granites in the Krušné hory/Erzgebirge Mts.; Central Europe. *Lithos* **2012**, *151*, 105–121. [CrossRef]
12. Gomes, M.; Neiva, A. Petrogenesis of tin-bearing granites from Ervedosa, northern Portugal: The importance of magmatic processes. *Chem. der Erde-Geochem.* **2002**, *62*, 47–72. [CrossRef]
13. Raimbault, L.; Cuney, M.; Azencott, C.; Duthou, J.; Joron, J.L. Geochemical evidence for a multistage magmatic genesis of Ta-Sn-Li mineralization in the granite at Beauvoir, French Massif Central. *Econ. Geol.* **1995**, *90*, 548–576. [CrossRef]
14. Kelly, W.C.; Rye, R.O. Geologic, fluid inclusion, and stable isotope studies of the tin-tungsten deposits of Panasqueira, Portugal. *Econ. Geol.* **1979**, *74*, 1721–1822. [CrossRef]
15. Siegel, K.; Williams-Jones, A.E.; Van Hinsberg, V.J. The amphiboles of the REE-rich A-type peralkaline Strange Lake pluton—Fingerprints of magma evolution. *Lithos* **2017**, *288*, 156–174. [CrossRef]
16. Khoshnoodi, K.; Behzadi, M.; Gannadi-Maragheh, M.; Yazdi, M. Alkali Metasomatism and Th-REE Mineralization in the Choghart deposit, Bafq district, Central Iran. *Geol. Croat.* **2017**, *70*, 53–69. [CrossRef]
17. Beus, A.A.; Severov, A.S.; Sitin, A.A.; Subbotin, K.D. *Albitized and Greisenized Granites (Apogranites)*; The USSR Academy of Sciences: Moscow, Russia, 1962; 193p. (In Russian)
18. Neiva, A. Portuguese granites associated with Sn-W and Au mineralizations. *Bull.-Geol. Soc. Finl.* **2002**, *74*, 79–101. [CrossRef]
19. Taylor, B.E.; O'Neil, J.R. Stable isotope studies of metasomatic Ca-Fe-Al-Si-skarns and associated metamorphic and igneous rocks Osgood mountains, Nevada. *Contrib. Mineral. Petrol.* **1977**, *63*, 1–50. [CrossRef]
20. Burtseva, M.V.; Ripp, G.S.; Posokhov, V.F.; Murzintseva, A.E. Nephrites of East Siberia: Geochemical features and problems of genesis. *Russ. Geol. Geophys.* **2015**, *56*, 516–527. [CrossRef]

21. Broom-Fendley, S.; Heaton, T.; Wall, F.; Gunn, G. Tracing the fluid source of heavy REE mineralisation in carbonatites using a novel method of oxygen-isotope analysis in apatite: The example of Songwe Hill, Malawi. *Chem. Geol.* **2016**, *440*, 275–287. [CrossRef]
22. Johnson, T.M.; Ripley, E.M. Hydrogen and oxygen isotopic systematic of berillium mineralisation Spor Mauntain, Utah. *Geol. Soc. Am. Abstr. Progr.* **1998**, *30*, 127.
23. Christiansen, E.H.; Bikun, J.V.; Sheridan, M.F.; Burt, D.M. Geochemical evolution of topaz rhyolites from the Thomas Range and Spor Mountain, Utah. *Am. Mineral.* **1984**, *69*, 223–236.
24. Sheglov, A.D. *Fundamentals of Metallogenic Analysis*; Nedra: Moscow, Russia, 1976; 295p. (In Russian)
25. Baturina, E.E.; Ripp, G.S. *Mo-W Deposits of the Western Transbaikalia*; Nauka: Moscow, Russia, 1984; 152p. (In Russian)
26. Ripp, G.S. *Geochemistry of Endogenous Mineralization and Forecasting Criteria in Folded Regions*; Nauka: Moscow, Russia, 1984; 192p. (In Russian)
27. Kushnarev, M.P. *The Structure of the Dzhida Deposit*; Academy of Sciences of the USSR: Moscow, Russia, 1954; 140p. (In Russian)
28. Ignatovich, V.I. Mineral and raw materials base of molybdenum. *Razvedka I ohrana nedr* **2007**, *12*, 37–43. (In Russian)
29. Povilaitis, M.M. *Endogenous Deposits of Tungsten and the Conditions for Their Formation*; Nedra: Moscow, Russia, 1979; 152p. (In Russian)
30. Ontoev, D.O. *Stages of Mineralization and Zoning of the Deposits of Transbaikalia*; Nauka: Moscow, Russia, 1974; 244p. (In Russian)
31. Pokalov, V.T. Age and geotectonics, the position of W-Mo mineralization in the Dzhida region of the Western Transbaikalia. *Dokl. Earth Sci.* **1979**, *247*, 678–681.
32. Ivanova, G.F.; Smirnova, O.K.; Ignatenko, K.I. Chemical composition of the wolframite-mineralization of the Dzhida ore field. *Zap. Russ. Mineral. Soc.* **1991**, *4*, 77–88. (In Russian)
33. Borshchevsky, Y.A.; Apeltsin, F.R.; Borisova, S.L. Isotope composition of oxygen of wolframite from tungsten deposits of various formation and genetic types. *Zap. Russ. Mineral. Soc.* **1980**, *4*, 633–643. (In Russian)
34. Platov, V.S.; Savchenko, A.A.; Ignatov, A.M.; Gorokhovsky, D.V. *State Geological Map of the Russian Federation*; Scale 1: 1000000 (Third Generation) Aldan-Transbaikalian Series; M-48. Ulan-Ude; VSEGEI: St. Petersburg, Russia, 2009; 271p. (In Russian)
35. Shapenko, V.V. Genetic features of tungsten mineralization of the Dzhida ore field (South-Western Transbaikalia). *Geol. Ore Depos.* **1982**, *5*, 18–29.
36. Reyf, F.G. *Ore-Forming Potential of Granites and Conditions for Its Realization*; Nauka: Moscow, Russia, 1990; p. 180. (In Russian)
37. Coplen, T.B. Normalization of oxygen and hydrogen data. *Chem. Geol.* **1988**, *72*, 293–297.
38. Friedman, I.; O'Neil, J.; Cebula, G. Two new carbonate stable isotope standards. *Geostand. Newsl.* **1982**, *6*, 11–12. [CrossRef]
39. Beaudoin, G.; Therrien, P. The updated web stable isotope fractionation calculator. In *Handbook of Stable Isotope Analytical Techniques*; Groot, P.A., Ed.; Elsevier: Amsterdam, The Netherlands, 2009; pp. 1120–1122.
40. Zhang, X.P.; Yao, T.D. World spatial characteristics of oxygen isotope ratio in precipitation. *J. Glaciol. Geocryol.* **1994**, *16*, 202–210.
41. Zheng, Y.-F. Oxygen isotope fractionation in wolframite. *Eur. J. Mineral.* **1992**, *4*, 1331–1335. [CrossRef]
42. Zheng, Y.-F. Calculation of oxygen isotope fractionation in anhydrous silicate minerals. *Geochim. Cosmochim. Acta* **1993**, *57*, 1079–1091. [CrossRef]
43. Zheng, Y.-F. Calculation of oxygen isotope fractionation in hydroxyl-bearing silicates. *Earth Planet. Sci. Lett.* **1993**, *120*, 247–263. [CrossRef]
44. Vennemann, T.W.; O'Neil, J.R. A simple and inexpensive method of hydrogen isotope and water analyses of minerals and rocks based on zinc reagent. *Chem. Geol. (Isot. Geosci. Sect.)* **1993**, *103*, 227–234. [CrossRef]
45. Grinenko, V.A. Preparation of sulfur dioxide for isotopic analysis. *Inorg. Chem.* **1962**, *7*, 2478–2482. (In Russian)
46. Savatenkov, V.M.; Morozova, I.M.; Levsky, L.K. Behavior of the Sm-Nd, Rb-Sr, K-Ar, and U-Pb isotopic systems during alkaline metasomatism: Fenites in the outer-contact zone of an ultramafic-alkaline intrusion. *Geochem. Int.* **2004**, *10*, 899–920.

47. Wickham, S.M.; Alberts, A.D.; Zanvilevich, A.N.; Litvinovsky, B.A.; Bindeman, J.N.; Schanble, E.A. A stable Isotope Study of Anorogenic Magmatism in East Central Asia. *Petrology* **1996**, *37*, 1063–1095. [CrossRef]
48. Litvinovsky, B.A.; Tsygankov, A.A.; Jahn, B.M.; Katzir, Y.; Be'eri-Shlevin, Y. The Late Paleozoic post-collisional igneous province of Transbaikalia (Russia). *Lithos* **2011**, *125*, 845–874. [CrossRef]
49. Tsygankov, A.A. Late paleozoic granitoids in Western Transbaikalia: Sequence of formation, sources of magmas, and geodynamics. *Russ. Geol. Geophys.* **2014**, *2*, 153–176. [CrossRef]
50. Taylor, H.P.; Frechen, J.; Degens, E.T. Oxygen and carbon isotope studies of carbonatites from the Laacher See district, West Germany and the Alno district, Sweden. *Geochim. Cosmochim. Acta* **1967**, *31*, 407–430. [CrossRef]
51. Yang, J.; Barling, J.; Siebert, C.; Fietzke, J.; Stephens, E.; Halliday, A.N. The molybdenium isotopic compositions of I-S and A-type granitic suites. *Geochim. Cosmochim. Acta* **2017**, *205*, 168–186. [CrossRef]
52. Hoefs, J. *Stable Isotope Geochemistry*; Springer-Verlag: Berlin/Heidelberg, Germany, 2009; 286p.
53. Letnikov, F.A. Fluid regime of endogenic proceces and ore-formation processes. *Russ. Geol. Geophys.* **2006**, *47*, 1296–1308.
54. Chukhrov, F.V.; Ermilova, L.P.; Vinogradov, V.I. *Isotopic Composition and Origin of Sulfur of Some Tungsten Deposits in Central Kazakhstan. Isotopes of Sulfur and Ore Formation*; Nauka: Moscow, Russia, 1987; pp. 46–58. (In Russian)
55. Borovikov, A.A.; Borisenko, A.S.; Shabalin, S.I.; Goverdovskiy, V.A.; Bryanskiy, N.V. Composition and metal contents of ore-forming fluids of the Kalguty Mo-W(Be) deposit (Gorny Altai). *Russ. Geol. Geophys.* **2016**, *4*, 507–518. [CrossRef]